




Thermal Annealing and Laser Treatment of Sol-gel Derived Zirconia Thin Films

Rainer Jahn¹ · Sönke Steenhusen¹ · Peer Löbmann¹ 

Accepted: 24 April 2020 / Published online: 6 May 2020
© The Author(s) 2020

Abstract

Soluble precursor powders were prepared from zirconium propoxide and acetylacetone by evaporation of volatile products directly after the hydrolysis step. Dissolution of the solid residue resulted in solutions that were further processed by dip coating on glass substrates. One set of asdried films was thermally annealed in an oven at temperatures between 300 and 600°C. In parallel, samples were irradiated by a CO₂ laser, in doing so laser power density and beam feed rate were varied. The thermally cured and laser treated film series were characterized with respect to film thickness, refractive index, phase content, crystallite size and film microstructure.

Keywords ZrO₂ · Thin films · Thermal curing · Laser processing · Microstructure

Introduction

The preparation of inorganic thin films by sol-gel processing has proven to be a flexible and cost-efficient alternative to vacuum-based technologies such as sputtering [1, 2]. The development of wet-chemical coating solutions with a sufficient stability under industrial conditions, however, is a challenging task. In this context the use of soluble precursor powders has been established for film compositions ranging from Al₂O₃ [3], TiO₂ [4], ZrO₂ [5] to lead zirconate titanate (PZT) [6]. As usual for such inorganic compositions film densification and crystallization were performed by thermal annealing.

As an alternative to oven treatment, sol-gel derived films may be annealed by irradiation with a laser source. Different lasers such as ArF [7, 8], KrF [7, 9–14], HeCd [15] and frequency tripled NdYAG [16, 17] operating at wavelengths below 1 μm have been used. In these cases, selective energy transfer to the film material is assumed which may enable the use of polymer substrates that may not withstand thermal sintering above 150°C. Even though this objective is commonly claimed, in most of

✉ Peer Löbmann
peer.loebmann@isc.fraunhofer.de

¹ Fraunhofer-Institut für Silicatforschung, Neunerplatz 2, 97082 Würzburg, Germany

the above studies inorganic substrates were used. This is so because organic residues were removed from the films by thermal treatment up to 500°C before the final laser irradiation.

For sintering of sol-gel films on glass and silica substrates the use of CO₂ lasers with a wavelength of 10,6 μm has been reported [18–21]. As these glasses strongly absorb in this spectral range [22, 23], an indirect heating of the above sol-gel films can be assumed. The local temperatures may well exceed the respective softening point of the glass substrate. Therefore, crystal phases that are not accessible by oven treatment may become accessible [19, 24–26].

In a previous publication [27] we systematically compared the CO₂ laser treatment of TiO₂ films derived from soluble precursor powders to parallel thermal annealing experiments. Laser power density could well be correlated to furnace temperatures in terms of film thickness and refractive index. However, whereas conventional thermal heating resulted in the anatase phase, exclusively rutile was found in films after laser treatment. In this manuscript we extend these systematic investigations to sol-gel derived coatings of zirconia (ZrO₂) composition.

Experimental Procedure

Film Preparation

Soluble ZrO₂ precursor powders were prepared similar to a procedure previously established for TiO₂ [4, 27]: By slow addition of 103,5 g (1.0 mol) acetylacetone to 485,6 g (1.0 mol) zirconium (IV)-propoxide a clear honey yellow solution was obtained which was heated up to 80°C for one hour. Subsequently, 54.0 g (3.0 mol) deionized water was added. Without any further delay all volatile components were separated from the reaction mixture by rotational evaporation at reduced pressure (< 40 mbar) with a maximum bath temperature of 80°C.

The coating solution was prepared by dissolution of this amorphous precursor powder in a mixture of 90 mass % ethanol and 10 mass % 1,5-pentanediol to result in an oxide yield of 6 mass % respective to crystalline ZrO₂. After stirring for 12 h it was filtered through a 0.45 μm membrane.

Thin films were deposited by dip coating of borosilicate glass (Schott, Borofloat®, 3.3 * 100 * 100 mm³) that was pre-cleaned in a laboratory dishwasher using an alkaline detergent. Coating experiments were performed within 8 h after cleaning. Directly before film deposition the substrates were additionally cleaned with compressed air.

Thin film preparation was carried out in clean room atmosphere at 24°C. The coating was made with a withdrawal rate resulting in a film thickness of 120 nm after sintering at 600°C. The as-coated plates remained in a fume hood for at least two minutes before they were dried in a vented furnace at 80°C for one hour.

Thermal Annealing

Directly after the drying, calcinations of the sol-gel films were achieved by rapid thermal annealing (RTA) for 10 min using a vented oven pre-heated to temperatures between 300 and 600°C).

Laser Treatment

The films dried at 80°C were shipped from Fraunhofer ISC Würzburg to LZH Hanover where laser treatment was performed. A CO₂ laser with the wavelength of 10,6 μm (Firestar ti-60, Synrad, Inc.) with a maximum power of 35 W was used. The quasi-continuous mode operated with a repetition rate of 10 kHz. The beam with a diameter of approximately 200 μm was focused on the samples by a galvanometer scanner and a f-theta lens with a focal length of 324 mm. Feed rates ranging from 500 mm/s to 3000 mm/s and a hatch of 200 μm between the laser lines were applied. Using these parameters the laser power density was varied between 64 W/mm² and 605 W/mm² by varying the duty cycle.

Material Characterization

Reflection curves were measured with a UV-Vis-spectrometer (Shimadzu UV-3100, Kyoto, Japan) in the range of 300 nm – 1700 nm. Analysis of the single layers was achieved using the Fresnel equations for vertical incidence and the interference law. So refractive index and layer thickness could be calculated by regarding the evaluable extremes of reflection. Details about this technique can be found in [28].

The films were characterized by X-ray diffractometry (XRD; Empyrean, Malvern Panalytical Ltd, United Kingdom) with regard to phase development. Grazing incidence X-ray diffractometry was performed at an incidence angle of 1°. Crystallite sizes were calculated using the Scherrer equation.

For microstructural analysis, scanning electron microscopy (SEM), (Supra 55VP, Carl Zeiss AG, Oberkochen, Germany) was used. Some samples were mechanically fractured in order to take images of cross-sections. All specimen were sputtered with platinum prior to the examination.

Results and Discussion

Thin films in ZrO₂ composition were deposited on borosilicate glass substrates by dip coating. After thermal annealing their thickness and refractive index was measured. From Fig. 1 it can be seen that up to 450 ° a steady consolidation from 350 nm to 125 nm is induced, up to 600°C a constant level is maintained. In parallel the refractive index of the film rises from 1,55 to 1,95 as the annealing temperature is increased.

In Fig. 1b the SEM cross-sectional view of a ZrO₂ coating that had been thermally annealed at 600°C is given. The granular microstructure is very similar to those of its alumina [3] and titania [27, 29] counterparts. Obviously, despite their different compositions and crystallinity sol-gel processing of soluble precursor powders results in comparable textural film features.

With a constant feed rate of 500 mm/s the laser power density was varied for the irradiation of ZrO₂ films that only had undergone drying at 80°C. In Fig. 2a the resulting film thickness is given along with the values for the parallel thermal treatment experiments. The course of the respective data can well be correlated with each other: For a laser power density of 65 W/mm² the shrinkage is similar to samples that only had been dried at 80°C. For 415 W/mm² a densification equal to thermal annealing at

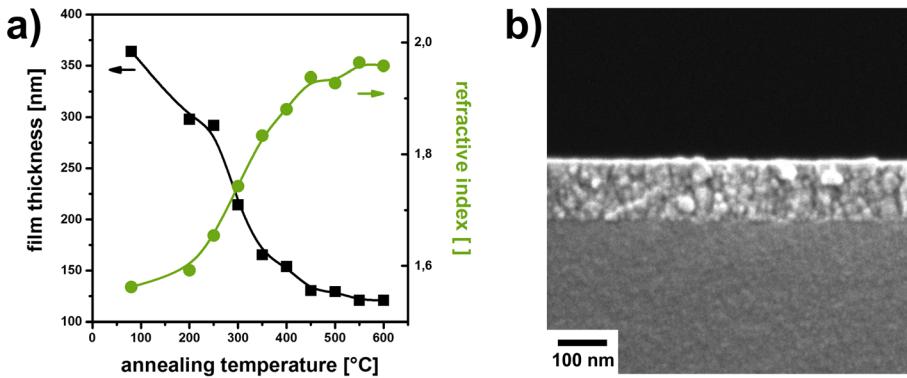


Fig. 1 Film thickness and refractive index of ZrO_2 films after thermal annealing (a) and SEM cross-sectional view of sample annealed at 600°C (b). See text for details

600°C is observed. For the evaluation of the refractive index (Fig. 2b) a similar good correspondence between the two experimental series can be seen: Values of 1,95 are measured for a laser power density of 415 W/mm^2 corresponding to annealing temperatures of 500 to 600°C .

It has to be emphasized that the laser irradiation in our study is done on as-dried sol-gel coatings and the removal of residual organics as well as densification/crystallization is done in a single irradiation step. In contrast to that most of the previous reports in the literature perform laser sintering on coatings that had experienced pre-treatment in a furnace at temperatures between 300 and 500°C [7, 10, 15, 17, 19, 20, 25, 26].

X-ray diffraction (XRD) experiments were performed on the films in order to determine the crystal phases present. After furnace treatment (Fig. 3a) up to 400°C the coatings remain amorphous, at 450°C first diffraction pattern corresponding to the tetragonal phase of ZrO_2 become apparent. At 500°C the peak intensity increases, above 550°C a saturation is observed. No monoclinic ZrO_2 is observed which corresponds to other sol-gel derived

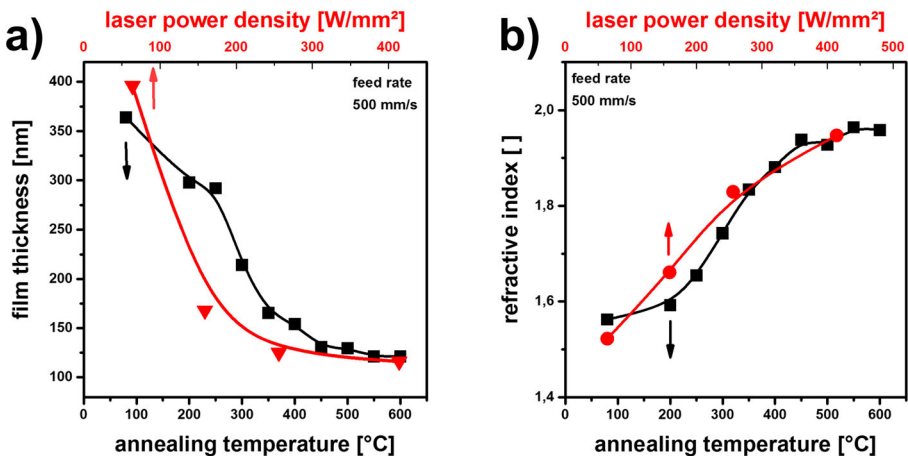


Fig. 2 Thickness (a) and refractive index (b) of ZrO_2 films that had undergone thermal annealing (black) and laser treatment (red). The feed rate was fixed at 500 mm/s whereas the laser power density was varied

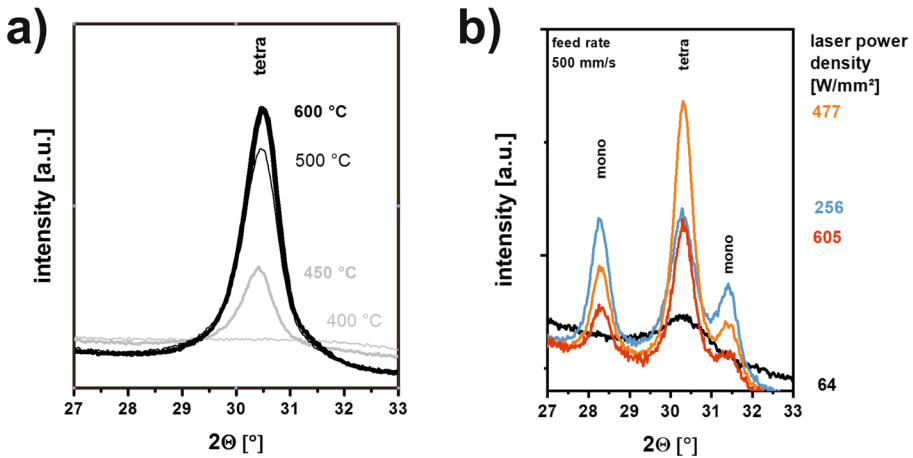


Fig. 3 X-ray diffraction pattern of ZrO_2 films after thermal annealing (a) and samples that had undergone CO_2 laser treatment (b) with the feed rate fixed at 500 mm/s and laser power rates as indicated

coatings after annealing at 500°C [30]. In contrast to that report, however, our films remain free from cracks throughout thermal processing.

Laser treatment at 64 W/mm² results in the first appearance of tetragonal ZrO_2 (Fig. 3b), above that laser power density this phase coexists with monoclinic ZrO_2 . The appearance of this thermodynamically more stable modification takes place in sol-gel derived films at temperatures exceeding 600°C [31, 32]. It therefore can be concluded that the local temperatures during laser sintering well exceed 600°C as suggested by theoretical simulations [19, 23] where surface temperatures exceeding 1000°C were calculated. In addition, it has been found that the crystallization of monoclinic ZrO_2 is favored by high heating rates [33].

As an intermediate result, it has to be noted, that different crystalline phases and thus differences in microstructure result from thermal annealing and CO_2 laser treatment, even though the film thickness and refractive index (Fig. 2) on first sight suggested matchable trends.

In our previous investigation on TiO_2 films, a similar behavior was observed: Laser treatment resulted solely in formation of the thermodynamically stable rutile phase, whereas in conventional thermal annealing only phase-pure anatase was found [27].

It appears from Fig. 3b that the peak intensity decreases when the laser power density is raised to 605 W/mm². This observation may indicate the removal of film material by ablation at high energies as previously reported [34].

The crystal sizes as calculated from the peak width of Fig. 3 by the Scherrer equation are given in Fig. 4. Thermal annealing between 500 and 600°C results in crystallites of tetragonal ZrO_2 with sizes between 15 nm and 20 nm. These diameters basically conform to the size of granular structures found in Fig. 1b. For laser annealing with power densities below 300 W/mm² tetragonal grains in the same order of magnitude are found. Above 300 W/mm² tetragonal and monoclinic ZrO_2 coexist with grain sizes exceeding the values measured for films that had undergone thermal treatment. This observation supports the assumption that the local temperatures during laser irradiation significantly exceed 600°C.

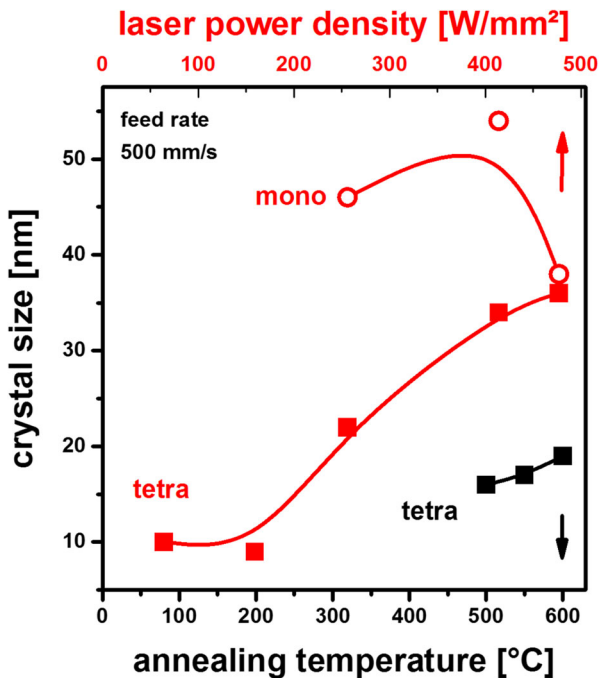


Fig. 4 Crystal size of ZrO_2 films after thermal annealing (black) and samples that had undergone CO_2 laser treatment (red) with different laser power density. The laser feed rate was fixed at 500 mm/s

For a given laser power density the beam feed rate determines the photon fluence, in a manner of speaking the local energy input to the substrate: The faster a given beam traverses, the smaller the power delivered to the surface.

With a power density of 414 W/mm^2 and a feed rate of 500 mm/s a film densification similar to that of thermal sintering at 600°C was obtained (Fig. 2). With this given power output the feed rate of the laser beam was varied from 500 mm/s to 4000 mm/s. In Fig. 5a the resulting ZrO_2 film thickness is compared to that resulting from conventional furnace processing. It can be seen that the laser irradiation can precisely emulate the thermal film densification. The same applies for the refractive index of the ZrO_2 coatings (Fig. 5b).

XRD phase analysis was performed on this sample series. From Fig. 6a it can be seen that a feed rate of 500 mm/s results in a certain ratio of monoclinic to tetragonal reflex intensity, that is shifted to tetragonal ZrO_2 at higher feed rates. At 1500 mm/s the tetragonal phase is detected almost exclusively. Obviously, the energy input under these conditions does not facilitate the formation of the thermodynamically more stable monoclinic phase any more. When the feed rate is raised to 3000 mm/s, the diffraction signal corresponding to tetragonal ZrO_2 is transformed to a broad hump indicating a low level of crystallinity.

Crystallite size analysis reveals that for feed rates of 500 mm/s and 1000 mm/s tetragonal and monoclinic grains with diameters exceeding 30 nm coexist. For thermal treatment between 500 and 600°C only tetragonal crystallites with diameters between 15 nm and 20 nm were found.

Structural uniformity is a key feature for the technical application of thin films. In Fig. 7a representative SEM image for a laser-processed ZrO_2 film is given. In general, no distinctive border between adjacent laser lines (hatch 200 μm) can be distinguished.

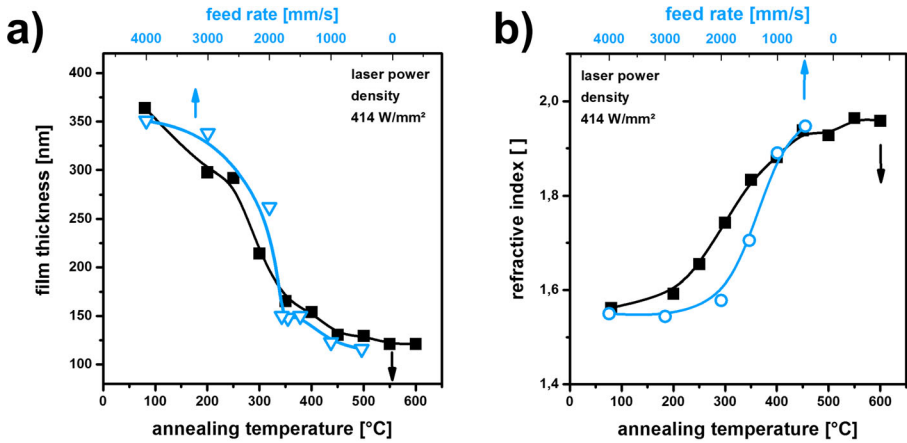


Fig. 5 Thickness (a) and refractive index (b) of ZrO₂ films that had undergone thermal annealing (black) and laser treatment (blue). The laser power density was fixed at 414 W/mm² whereas the beam feed rate was varied as indicated

Within the beam center, some defects are located inside a zone of 70 μm width. The cross-sectional view reveals that in this region the ZrO₂ film spans bubbles that extend into the substrate. The defects obviously result from partial flaking of such ZrO₂ film domes. This observation suggests that the glass substrate is substantially liquefied by the high temperatures that is induced by laser processing. The bubbles are presumably generated by gaseous products that result during the pyrolysis of the sol-gel film. Outside the central defective zone, however, the ZrO₂ film appears homogeneous and uniform similar to samples that have been thermally annealed (Fig. 1b).

Some similar features have been observed for laser-treated TiO₂ films previously studied [27]. In contrast to that report, however, no evidence for partial ZrO₂ removal

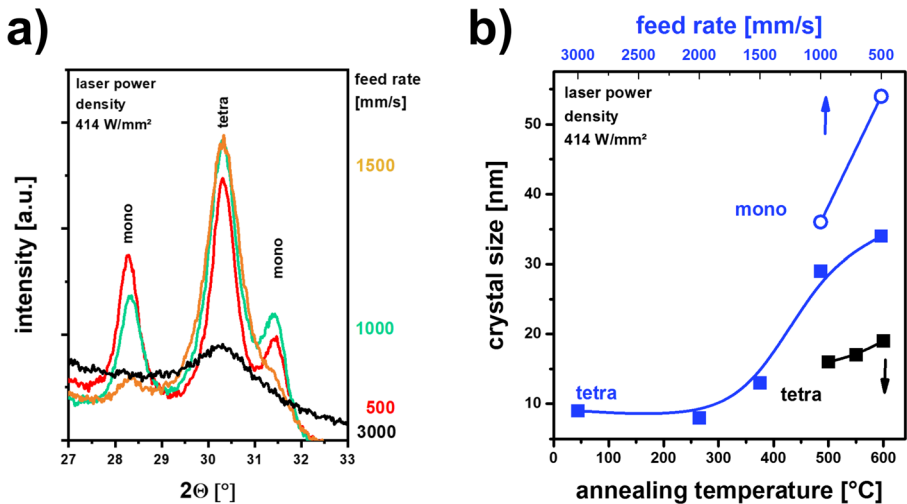


Fig. 6 X-ray diffraction pattern of ZrO₂ films treated with a laser power density fixed at 414 W/mm² and a beam feed rate varied as indicated (a). In (b) the resulting crystal sizes (blue) are compared to values observed after thermal annealing (black)

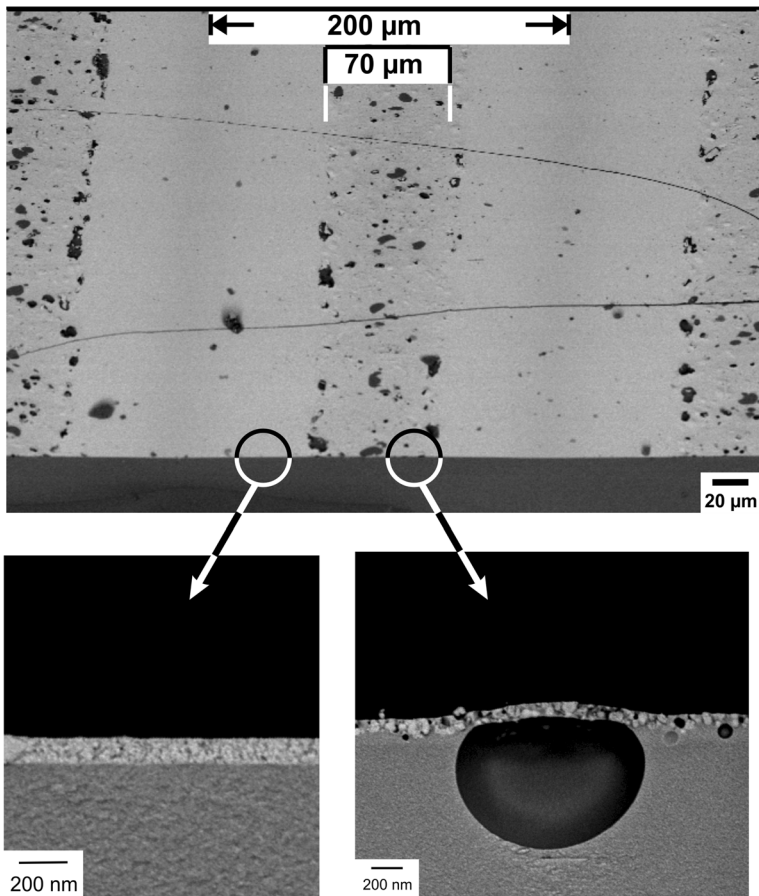


Fig. 7 SEM images of ZrO_2 film after CO_2 laser treatment with 415 J/mm^2 and a beam feed rate of 500 mm/s . In the **top** a fractured specimen with a tilt angle of 45° is shown, in the **bottom** part some representative images with a higher magnification are given

by ablation could be observed here even though identical laser parameters have been applied. In the whole the ZrO_2 material seems to be more damage resistant than TiO_2 [27].

Conclusions

ZrO_2 sol-gel coatings can successfully be processed by conventional thermal annealing and CO_2 laser treatment. Film properties such as film thickness, refractive index and grain size systematically correlate with laser power density and beam feed rate. Results indicate that laser irradiation locally induces substrate temperatures by far exceeding 600°C that lead to the coexistence of the monoclinic and tetragonal phase of ZrO_2 .

Acknowledgements This work was funded by the Federal Ministry for Economic Affairs and Energy (IGF grant 19454N project “LASIP”). The authors thank Laserzentrum Hannover (LZH) for the laser processing of the sol-gel films.

Funding Information Open Access funding provided by Projekt DEAL.

Compliance with Ethical Standards

Conflict of Interest The authors declare that they have no competing interests.

Open Access This article is licensed under a Creative Commons Attribution 4.0 International License, which permits use, sharing, adaptation, distribution and reproduction in any medium or format, as long as you give appropriate credit to the original author(s) and the source, provide a link to the Creative Commons licence, and indicate if changes were made. The images or other third party material in this article are included in the article's Creative Commons licence, unless indicated otherwise in a credit line to the material. If material is not included in the article's Creative Commons licence and your intended use is not permitted by statutory regulation or exceeds the permitted use, you will need to obtain permission directly from the copyright holder. To view a copy of this licence, visit <http://creativecommons.org/licenses/by/4.0/>.

References

1. Chemical solution deposition of functional oxide thin film. In: Schneller, T., Waser, R., Kosec, M., Payne, D. (eds.) Springer, Wien (2013)
2. Handbook of Sol-Gel Science and Technology. In: Klein, L. et al. (eds.) Springer International Publishing, Switzerland (2016)
3. Müller, K., Hegmann, J., Jahn, R., Löbmann, P.: Adjustable refractive index of titania–alumina thin films prepared from soluble precursor powders. *J. Sol-Gel. Sci. Technol.* **77**(1), 69–77 (2016). <https://doi.org/10.1007/s10971-015-3829-7>
4. Löbmann, P.: Soluble powders as precursors for TiO₂ thin films. *J. Sol-Gel. Sci. Technol.* **33**, 275–282 (2005). <https://doi.org/10.1007/s10971-005-6377-8>
5. Löbmann, P., Jahn, R., Seifert, S., Sporn, D.: Inorganic thin films prepared from soluble powders and their applications. *J. Sol-Gel. Sci. Technol.* **19**, 473–477 (2000)
6. Löbmann, P., Seifert, S., Merklein, S., Sporn, D.: Lead zirconate-titanate films prepared from soluble powders. *J. Sol-Gel. Sci. Technol.* **13**, 827–831 (1998)
7. Sandu, C.S., Teodorescu, V.S., Ghica, C., Canut, B., Blanchin, M.G., Roger, J.A., Brioude, A., Bret, T., Hoffmann, P., Garapon, C.: Densification and crystallization of SnO₂: Sb sol–gel films using excimer laser annealing. *Appl. Surf. Sci.* **208–209**, 382–387 (2003). [https://doi.org/10.1016/S0169-4332\(02\)01412-5](https://doi.org/10.1016/S0169-4332(02)01412-5)
8. Berkani, O., Latrous, K., El Hamzaoul, H., Bouazaoul, M., Capoen, B.: UV laser irradiation-induced crystallization in titania thick film prepared using sol-gel method. *JNTM* **2**(2), 13–17 (2012)
9. Nagase, T., Ooie, T., Sakakibara, J.: A novel approach to prepare zinc oxide films: Excimer laser irradiation of sol-gel derived precursor films. *Thin Solid Films.* **357**, 151–158 (1999). [https://doi.org/10.1016/S0040-6090\(99\)00645-8](https://doi.org/10.1016/S0040-6090(99)00645-8)
10. Tsang, W.M., Wong, F.L., Fung, M.K., Chang, J.C., Lee, C.S., Lee, S.T.: Transparent conducting aluminum-doped zinc oxide thin film prepared by sol–gel process followed by laser irradiation treatment. *Thin Solid Films.* **517**(2), 891–895 (2008). <https://doi.org/10.1016/j.tsf.2008.08.157>
11. Joya, Y.F., Liu, Z.: Effect of the excimer laser irradiation on sol–gel derived tungsten–titanium dioxide thin films. *Appl. Phys. A.* **102**(1), 91–97 (2011). <https://doi.org/10.1007/s00339-010-6151-9>
12. Joya, Y.F., Liu, Z., Wang, Z.: Generation of silver-anatase nanocomposite by excimer laser-assisted processing. *AIP Adv.* **2**(032171), 1–8 (2012). <https://doi.org/10.1063/1.4754284>
13. Tsay, C.-Y., Huang, T.-T.: Characterization of low-temperature solution-processed indium–zinc oxide semiconductor thin films by KrF excimer laser annealing. *Ceram. Int.* **40**(6), 8287–8292 (2014). <https://doi.org/10.1016/j.ceramint.2014.01.030>
14. Dellis, S., Isakov, I., Kalfagiannis, N., Tetzner, K., Anthopoulos, T.D., Koutsogeorgis, D.C.: Rapid laser-induced photochemical conversion of sol-gel precursors to In₂O₃ layers and their application in thin-film transistors. *J. Mater. Chem. C.* **5**, 3673–3677 (2017). <https://doi.org/10.1039/c7tc00169>
15. Su Kim, M., Kim, S., Leem, J.-Y.: Laser-assisted sol-gel growth and characteristics of ZnO thin films. *Appl. Phys. Lett.* **100**, 252108 (2012). <https://doi.org/10.1063/1.4729944>

16. Langlade, C., Vannes, B., Sarnet, T., Autric, M.: Characterization of titanium oxide films with Magneli structure elaborated by sol-gel route. *Appl. Surf. Sci.* **186**, 145–149 (2002). [https://doi.org/10.1016/S0169-4332\(01\)00642-0](https://doi.org/10.1016/S0169-4332(01)00642-0)
17. Al-Asedy, H.J., Al-Khafaji, S.A., Bakhtiar, H., Bidin, N.: Properties of Al- and Ga-doped thin zinc oxide films treated with UV laser radiation. *Appl. Phys. A.* **124**(3), 223 (2018). <https://doi.org/10.1007/s00339-018-1619-0>
18. Pütz, J., Ganz, D., Gasparo, G., Aergeter, M.A.: Influence of the Heating Rate on the Microstructure and on Macroscopic Properties of Sol-Gel SnO₂: Sb Coatings. *J. Sol-Gel. Sci. Technol.* **13**, 1005–1010 (1998)
19. Baber, J., Raether, F.: Production of oxide ceramic coatings on glass by laser sintering. *Glass Sci. Technol.* **73**(7), 211–214 (2000)
20. Jiwei, Z., Liangying, Z., Xi, Y., Hofsgon, S.N.B.: Characteristics of laser-densified and conventionally heat treated sol-gel derived silica-titania films. *Surf. Coat. Technol.* **138**, 135–140 (2001). [https://doi.org/10.1016/S0257-8972\(00\)01158-0](https://doi.org/10.1016/S0257-8972(00)01158-0)
21. Chou, C.-C., Tsai, S.-D., Tu, W.-H., Yeh-Liu, Y.-E., Tsai, H.-L.: Low-temperature processing of sol-gel derived Pb(Zr,Ti)O₃ thick films using CO₂ laser annealing. *J. Sol-Gel. Sci. Technol.* **42**(3), 315–322 (2007). <https://doi.org/10.1007/s10971-007-0768-y>
22. Buerhop, C., Blumenthal, B., Weissmann, R., Lutz, N., Biermann, S.: Glass surface treatment with excimer and CO₂ lasers. *Appl. Surf. Sci.* **46**, 430–434 (1990). [https://doi.org/10.1016/0169-4332\(90\)90184-2](https://doi.org/10.1016/0169-4332(90)90184-2)
23. Wang, X., Jiao, J., Lu, H.: Temperature and stress prediction for CO₂ laser heating glass plate, Gmunden, Austria, pp. 1–6. SPIE, Bellingham (2006). <https://doi.org/10.1117/12.739389>
24. Chung, C.K., Chuang, K.P., Cheng, S.Y., Lin, S.L., Hsie, K.Y.: Effect of solution contents on the evolution of microstructure and photoluminescence of laser-annealed rutile TiO₂ thin films. *J. Alloys Compd.* **574**, 83–87 (2013). <https://doi.org/10.1016/j.jallcom.2013.04.045>
25. Knite, M., Mezinskis, G., Shebanovs, L., Pedaja, I., Sternbergs, A.: CO₂ laser-induced structure changes in lead zirconate titanate Pb(Zr_{0.58}Ti_{0.42})O₃ sol-gel films, *Appl. Surf. Sci.* **208–209**, 378–381 (2003). [https://doi.org/10.1016/S0169-4332\(02\)01408-3](https://doi.org/10.1016/S0169-4332(02)01408-3)
26. Medina-Valtierra, J., Frausto-Reyes, C., Ortiz-Morales, M.: Phase transformation in semi-transparent TiO₂ films irradiated with CO₂ laser. *Mater. Lett.* **66**(1), 172–175 (2012). <https://doi.org/10.1016/j.matlet.2011.08.076>
27. Wesang, K., Hohnholz, A., Jahn, R., Steenhusen, S., Löbmann, P.: Systematic Comparison of Thermal Annealing and Laser Treatment of TiO₂ Thin Films Prepared by Sol-Gel Processing. *Lasers in Manufacturing and Materials Processing*, **6**, 387–397 (2019). <https://doi.org/10.1007/s40516-019-00101-2>
28. Schmitt, A., Bittner, A., Jahn, R., Löbmann, P.: Characterization of stacked sol-gel films: Comparison of results derived from scanning electron microscopy, UV-Vis spectroscopy and ellipsometric porosimetry. *ThinSolidFilms* **520**, 1880–1884 (2012). <https://doi.org/10.1016/j.tsf.2011.09.021>
29. Bittner, A., Jahn, R., Löbmann, P.: TiO₂ thin films on soda-lime and borosilicate glass prepared by sol-gel processing: Influence of the substrates. *J. Sol-Gel. Sci. Technol.* **58**(2), 400–406 (2011). <https://doi.org/10.1007/s10971-011-2406-y>
30. Jothi, S., Prithvikumaran, N., Jeyakumaran, N.: Optical parameter determination of ZrO₂ thin films prepared by sol gel dip coating. *International Journal of ChemTech Research* **6**, 5342–5346 (2014)
31. Li, H., Liang, K., Gu, S., Xiao, G.: Oriented nano-structured ZrO₂ thin films on fused quartz substrate by sol-gel process. *Journal of Materials Science Letters*. **20**, 1301–1303 (2001). <https://doi.org/10.1023/A:1010938215228>
32. Shimizu, H., Konagai, S., Ikeda, M., Nishide, T.: Characterization of Sol-Gel Derived and Crystallized ZrO₂ Thin Films. *Jpn. J. Appl. Phys.* **48**, 101101 (2009). <https://doi.org/10.1143/JJAP48.101101>
33. Kogler, M., Köck, E., Vanicek, S., Schmidmair, D., Götsch, T., Stoöger-Pollach, M., Hejny, C., Klötzer, B., Penner, S.: Enhanced Kinetic Stability of Pure and Y-Doped Tetragonal ZrO₂. *Inorg.Chem.* **53**, 13247–13257 (2014). <https://doi.org/10.1021/ic502623t>
34. Hawelka, D., Stollenwerk, J., Pirch, N., Wissenbach, K., Loosen, P.: Improving surface properties by laser-based drying, gelation, and densification of printed sol-gel coatings. *J. Coat. Technol. Res.* **11**(1), 3–10 (2014). <https://doi.org/10.1007/s11998-013-9516-0>